THE JOURNAL OF PHYSICAL CHEMISTRY B

Article

pubs.acs.org/JPCB

Packing Dependent Electronic Coupling in Single Poly(3-hexylthiophene) H- and J-Aggregate Nanofibers

Thomas P. Martin,[#,†] Adam J. Wise,[#,†] Erik Busby,[‡] Jian Gao,[†] John D. Roehling,[§] Michael J. Ford,[‡] Delmar S. Larsen,[‡] Adam J. Moulé,[§] and John K. Grey*[,†]

[†]Department of Chemistry and Chemical Biology, MSC03 2060, University of New Mexico, Albuquerque, New Mexico 87131, United States

[‡]Department of Chemistry, and [§]Department of Chemical Engineering, University of California—Davis, One Shields Avenue, Davis, California 95618, United States

Supporting Information

ABSTRACT: Nanofibers (NFs) of the prototype conjugated polymer, poly(3-hexylthiophene) (P3HT), displaying H- and J-aggregate character are studied using temperature- and pressure-dependent photoluminescence (PL) spectroscopy. Single J-aggregate NF spectra show a decrease of the 0−0/0−1 vibronic intensity ratio from ∼2.0 at 300 K to ∼1.3 at 4 K. Temperature-dependent PL line shape parameters (i.e., 0−0 energies and 0−0/0−1 intensity ratios) undergo an abrupt change in the range of ∼110—130 K suggesting a change in NF chain packing. Pressure-dependent PL lifetimes also show increased contributions from an instrument-limited decay component which is attributed to greater torsional disorder of the P3HT backbone upon decreasing NF volume. It is proposed that the P3HT alkyl side groups change their packing arrangement from a type I to type II configuration causing a decrease in J-aggregate character (lower intrachain order) in both temperature- and pressure-dependent PL spectra. Chain packing dependent exciton and polaron relaxation and recombination dynamics in NF aggregates are next studied using transient absorption spectroscopy (TAS). TAS data reveal faster polaron recombination dynamics in H-type P3HT NFs indicative of interchain delocalization whereas J-type NFs exhibit delayed recombination suggesting that polarons (in addition to excitons) are more delocalized along individual chains. Both time-resolved and steady-state spectra confirm that excitons and polarons in J-type NFs are predominantly intrachain in nature that can acquire interchain character with small structural (chain packing) perturbations.

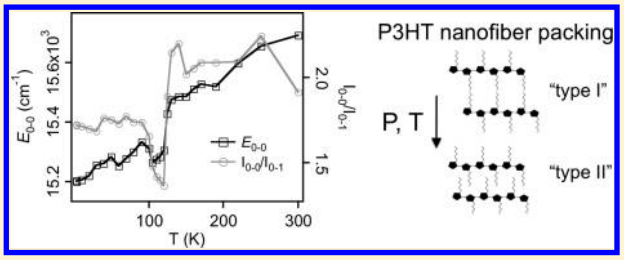

INTRODUCTION

Electronic coupling in π-stacked poly(3-hexylthiophene) (P3HT) aggregates shows a strong sensitivity to the conformation and packing characteristics of individual chains comprising the aggregate.[1−5] According to Spano and co-workers, when intrachain order (i.e., planarity of monomers within chain segments) is low, optical spectra resemble H-aggregates where the electronic origin (0−0) transition is less intense than the 0−1 vibronic sideband.[6] This is typically the case for solution-cast P3HT thin films due to polydispersity effects that lead to stacking faults within the aggregate and smaller aggregate sizes (∼10−30 nm).[7]

Self-assembly techniques have been introduced recently to form nanofibers (NFs) of P3HT aggregates which provide the ability to control aggregate size and ordering characteristics of constituent chains. By controlling the assembly process of P3HT aggregates through solvent−solute interactions, selective tuning of exciton coupling in the NF is also possible.[8−11] For example, intrachain order in the NF aggregates can be tuned by controlling the specific molecular weight fraction of the P3HT chains forming aggregates. This effect suppresses stacking faults thereby allowing substantial elongation and planarization of the P3HT chains. The result is that exciton coupling can be tuned between the H- and J-type exciton coupling limits although the latter rarely makes an appearance due to the requirement of high intrachain order. Niles et al. recently demonstrated J-aggregate behavior in P3HT NFs assembled in toluene solutions which, from assembly over long periods of time (∼24 h), form high quality aggregates with significant molecular weight fractionation.[12] This situation promotes unusually high intrachain order (chain planarity) and, likewise, the dominance of intrachain coupling over the more typical interchain term leading to H-aggregate character. Importantly, J-type P3HT aggregates are sensitive to seemingly minor changes in intrachain order such as temperature- and pressure-induced changes in packing (NF volume) that decrease intrachain order and restore H-type behavior.[12] This apparent delicate interplay between intrachain order and interchain coupling is reversible and allows electronic coupling in P3HT aggregates to be reliably tuned between the H- and J-type

Special Issue: Paul F. Barbara Memorial Issue

Received: August 29, 2012
Revised: December 1, 2012
Published: December 6, 2012

limits. Here, we use detailed temperature-, pressure- and polarization-dependent photoluminescence (PL) measurements on both H- and J-type single P3HT NF's to better understand the specific structural factors governing exciton coupling and their susceptibility to change with small perturbations to chain packing characteristics. Transient absorption spectroscopy (TAS) measurements are also performed on both H- and J-type NFs to obtain detailed correlations between the roles of chain packing and order on exciton and polaron relaxation and recombination dynamics preceding PL transitions.

The appearance of J-type behavior in P3HT aggregates is surprising but, it is important to note that these NFs do not behave as ideal J-aggregates but, rather, a hybrid between both ideal H- and J-type behavior. Theory predicts that aggregates with a small, but nonzero, interchain coupling should revert to H-type behavior when kT is smaller than this term (assuming no temperature-dependent changes in chain packing characteristics).[6] PL lineshapes of J-type P3HT NFs show a decrease in 0−0/0−1 ratios at low temperatures indicating a residual interchain coupling term.[12] This interchain contribution was estimated to be ∼50−100 cm^{-1}, much smaller than values obtained for thin films (∼300−400 cm^{-1}).[12] Conversely, pure J-aggregates show enhancements of the 0−0/0−1 ratios with $1/\sqrt{T}$ since interchain coupling goes to zero with high intrachain order.[13,14] Although the observed trends in J-type P3HT NFs are consistent with theoretical predictions, the aggregate model excludes the role of the alkyl side chains on the polymer backbone which may change their packing arrangement upon decreasing NF volume (viz. low temperature and high pressure). This is especially important for the J-aggregate NFs where even a small disruption of the alkyl chain packing could alter intrachain order and, consequently, exciton coupling. Our previous PL studies of these NFs were only measured at two temperatures making it difficult to determine if significant structural changes occur that disturb intrachain order and, in turn, destroy J-type behavior.

In the following we present detailed temperature-dependent PL data from well-dispersed single J-type P3HT NFs showing increased H-aggregate character at low temperatures as well as evidence for a structural phase transition in the range of ∼110−130 K. We propose that a change in packing of the P3HT alkyl side groups occurs that induces sufficient torsional disorder in the π-stacked P3HT chains thus lowering intrachain order. Pressure-dependent NF PL lifetimes are also measured that show increases of a fast (instrument-limited) decay component at higher pressures that is attributed to excited state interchain torsional relaxation. These trends are consistent with previous pressure-dependent PL spectra displaying reductions in J-aggregate character and indicate increase torsional disorder. J-type behavior is restored upon return of temperature and pressure to their ambient which is consistent with a minor change in chain packing.

Temperature-dependent PL spectra of H-type P3HT NFs assembled in either anisole or xylene are also investigated to verify if similar changes occur in chain packing characteristics and, hence, exciton coupling. Unlike their J-aggregate cousins, these NFs possess substantially larger disorder and interchain couplings and show comparatively little change over the temperature range studied (4−300 K). Unusual features, such as multiple electronic origins from different emitting species, also appear in low temperature PL spectra of single H-type NFs possibly arising from domains, or grains, with different chain packing characteristics.[15] The greater heterogeneity present in H-type NFs most likely arises from their rapid formation in solutions whereas J-type NFs form over longer periods of time leading to less stacking faults in the π-stacks.

Lastly, TAS was performed on H- and J-aggregate NF dilute solution suspensions to obtain a more complete photophysical picture of the influence of chain packing and order on ultrafast exciton relaxation[16,17] and autoionization[18,19] processes. TAS reveals similar exciton recombination dynamics for both structures but distinctly different polaron yield and recombination dynamics. For example, H-type structures exhibit high polaron yields and faster recombination dynamics representative of limited polaron delocalization along single chains within the aggregate, which is expected owing to the larger number of stacking faults present in H-aggregates. On the other hand, J-type NFs show substantially lower polaron yields and delayed recombination dynamics that are directly attributable to enhanced intrachain polaron delocalization. These findings are consistent with pictures borne out from steady state optical spectra where J-type NFs effectively behave as a collective of highly planarized P3HT chains that are nearly electronically isolated from each other despite the close distance between them.

EXPERIMENTAL SECTION

Single NF Spectroscopy. NF structures of regioregular P3HT (Plextronics, ∼98%) were self-assembled in various solvents depending on the desired exciton coupling characteristics of the aggregate using procedures described previously.[9] For example, anisole and xylene solutions result in similar H-type NFs whereas toluene solutions produce J-type structures. Samples for single NF PL imaging studies are prepared by dispersion into polystyrene host matrices and spin-coated onto clean glass coverslips to produce dilute thin films. The quality of NF samples was checked by optical absorption, PL and Raman spectroscopy. Upon processing, dilute NF thin films were placed inside an optical microscope cryostat (Oxford) and evacuated to ∼10^{-4} mbar. Samples were mounted on the cryostat coldfinger using Apiezon N cryogenic grease which also ensures good thermal contact. Single NFs were imaged using a home-built microscope spectrometer configured in a widefield geometry. Samples were illuminated using the unpolarized 514.5 nm line of an argon ion laser (Spectra Physics) or 568 nm line of a krypton ion laser (Melles-Griot) which showed identical PL lineshapes. Emitted light was filtered with long-pass edge filters (Semrock) and imaged onto the entrance slits of a liquid-nitrogen-cooled CCD spectrograph (Horiba/Jobin Yvon). To measure single NF spectra, slit widths were set to their minimum value enabling spectral acquisition of a single particle appearing on the entrance slits. All spectra were corrected for instrument response using a calibrated tungsten lamp and vibronic intensity ratios were determined from fitting Gaussian functions and using the integrated area under the curves. Polarized emission spectra were recorded by placing a polarizer in the path before the entrance slits of the monochromator followed by a polarization scrambler to minimize the polarization-dependent response of the grating. Excitation polarization-dependent PL imaging measurements were performed using either a polarizer and half-wave plate or electro-optical modulator controlled by the amplified signal of a function generator. Dye impregnated latex beads were used as a control to assess the degree of instrument depolarization effects.

dx.doi.org/10.1021/jp308586k | J. Phys. Chem. B 2013, 117, 4478−4487

Pressure-Dependent NF Lifetimes. Pressure-dependent PL lifetimes and spectra were recorded using a gas membrane driven diamond anvil cell on a confocal microscope spectrometer described in detail previously.[12] NF samples were dispersed in polystyrene and loaded into a prestressed steel gasket along with a methanol/water solution as the pressure-transmitting medium. PL spectra and lifetimes for a specific pressure were recorded simultaneously by using an optical (nonpolarizing, 50/50) beamsplitter that routes emitted photons to either a fast response avalanche photodiode (APD, idQuantique) for measuring lifetimes or a CCD spectrometer for measuring PL spectra. PL lifetimes were recorded using a time-correlated single photon counting module (Becker-Hickl) and decays were fitted using iterative convolution techniques with an instrument response function (IRF, ∼50 ps) generated using scattered excitation light from the diamond-anvil cell in the absence of the NF sample. Pressures were calibrated using the R1 peak of ruby.[20]

Transient Absorption Spectroscopy. Broadband ultrafast transient absorption spectroscopy (TAS) was conducted using a two-pulse pump−probe technique. The full experimental details of the setup can be found elsewhere,[21] and only the relevant details are provided below. Pump pulses were made via a noncollinear optical parametric amplifier pumped with the second harmonic of the 800 nm Ti:sapphire (Newport) fundamental. Supercontinuum probe pulses were generated by focused 800 nm fundamental into a rotating CaF_2 disc. Temporal delay between the pulses was introduced by mechanically delaying the probe light with a computer-controlled translation stage (Newport IMS600LM). The transmitted probe light was dispersed on to a 256 pixel silicon diode array (Hamamatsu S3901−256). Pump pulses were chopped at 500 Hz (Thorlabs MC100A).

RESULTS AND DISCUSSION

Temperature-Dependent Single NF Spectra. Figure 1 shows ensemble absorption and PL spectra of NF dispersions formed in anisole and toluene solutions (panels A and B). Comparison of the 0−0/0−1 absorption transitions produces values of <1 for the former and >1 for the latter indicating H- and J-type aggregates, respectively.[6] Corresponding PL spectra show 0−0/0−1 > 1 for both types of NF's with values of ∼2.0 for toluene and ∼1.3 for anisole assembled NFs. The appearance of weak J-aggregate character in the PL spectra of anisole NF dispersions is likely the result of energy transfer from the more plentiful H-type domains probably due to collapsed NF conformations in this poor solvent. The lower signal-to-noise ratios also demonstrate that J-type domains in anisole NFs are in fact minority emitters at the bottom of the energy funnel. This picture is further confirmed from PL excitation spectra of anisole NFs that show pronounced J-aggregate character (Figure 1A).

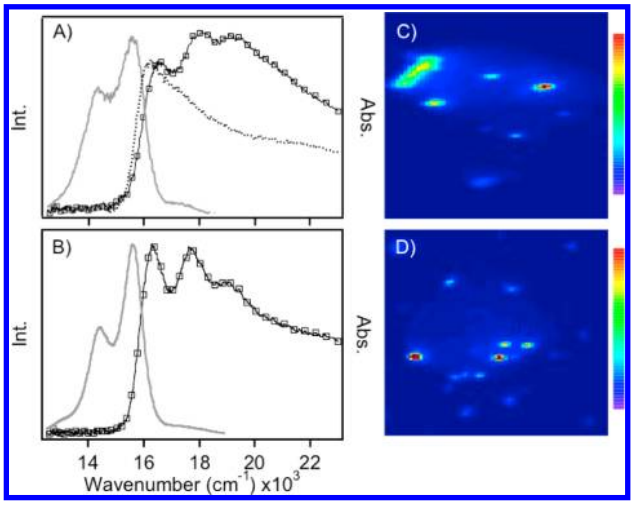

Figure 1. PL and absorption spectra of solution dispersions of anisole (A) and toluene (B) assembled P3HT NFs. A PL excitation spectrum (dotted trace) is also shown in (A) for anisole NFs. Representative widefield PL images of anisole (C) and toluene (D) NF's dispersed in polystyrene. Typical fields-of-view were ∼15 μm.

NFs were next dispersed into inert hosts, and single NF PL images and spectra were measured. Figure 1C,D shows typical widefield PL images from well-separated P3HT NFs, generally appearing as diffraction-limited spots. NF aspect ratios decrease upon dispersing into solid matrices, which was most prevalent for J-type NFs. Larger extended particles were observed in some cases, but spectral signatures were similar to smaller particles. Comparison of PL spectra from dispersed J-type NFs in either dilute solutions or polystyrene hosts also revealed identical line shape characteristics demonstrating no disruption of the aggregate chain packing upon dispersing into inert hosts. This was not the case for H-type NFs assembled in anisole where markedly different lineshapes were observed upon dispersion into solid matrices which is discussed in detail in the following. NFs exhibit no PL intermittency over the time scale of spectral acquisition (∼1−5 min), consistent with previous measurements performed on a scanning confocal microscope under nitrogen environments and similar excitation power densities (∼100 W/cm^2).[12] Variable temperature PL spectra from both single and ensemble NFs were next measured to further illuminate the interplay between intrachain order and interchain coupling.

A key finding from Niles et al. was that P3HT aggregates with nonzero interchain coupling should revert to H-type behavior at low temperatures, i.e., when kT is smaller than this coupling.[12] Figure 2 presents representative single NF spectra from J-type aggregate structures at several temperatures which show red-shifts of up to ∼500 cm^{-1} and 0−0/0−1 ratios decrease by almost a factor of 2 at ca. 4 K indicating increased interchain exciton bandwidths. Single NF vibronic linewidths showed no appreciable changes with temperature and an instrument artifact was also observed in single NF PL spectra appearing as a small dip at ∼13 800 cm^{-1}. The severity of this artifact varied from particle-to-particle and was caused by the polarization dependence of the spectrometer grating and microscope dichroic mirror.

Figure 3 shows temperature-dependent 0−0/0−1 intensity ratios and 0−0 energies (E_{0-0}) from an ensemble average response of several NFs measured over the microscope field-of-view (∼15 μm) (A) and a single NF (B) J-aggregate. In addition to the increased H-type behavior at lower temperatures, a discontinuity in the PL line shape parameters occurs at ∼110−130 K that was not observed previously due to the limited temperature range used.[12] This feature was most prominent in single NF spectra since ensemble spectra are averaged over several local NF environments. Similar behavior was observed for different cooling/heating rates demonstrating that the transition is not caused by a phase transition or disruption (fracturing) of the polystyrene matrix or change in the specific heat capacity of the cryogenic grease used.

dx.doi.org/10.1021/jp308586k | J. Phys. Chem. B 2013, 117, 4478−4487

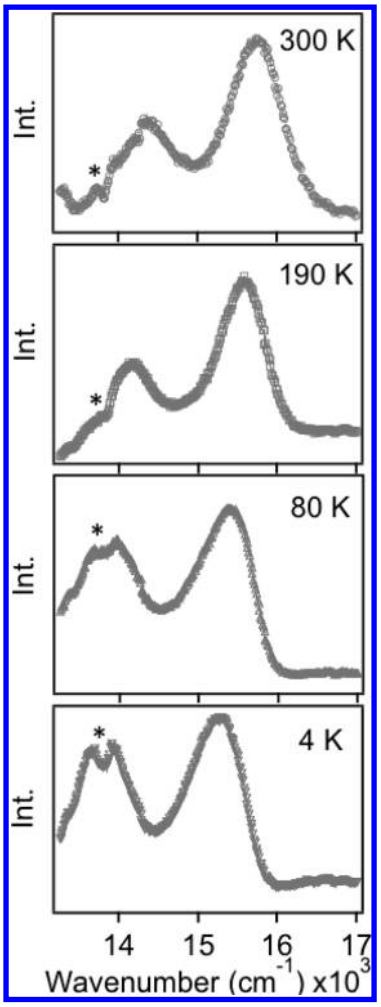

Figure 2. Representative PL spectra of toluene assembled P3HT NFs at several temperatures. * denotes a grating/dichroic polarization artifact only apparent in single NF spectra.

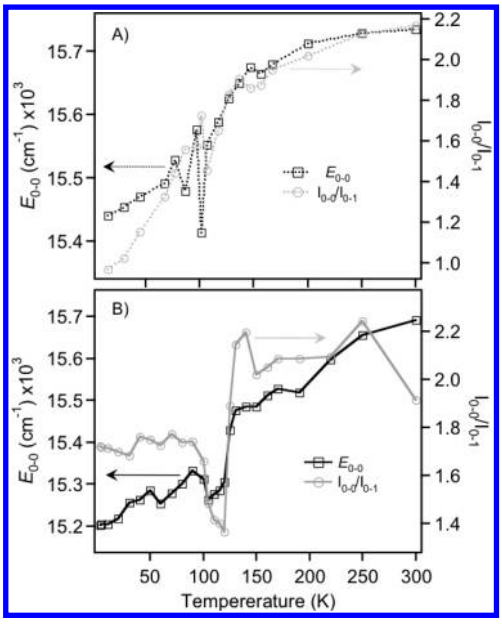

Figure 3. Temperature-dependent PL 0−0/0−1 ratios and E_{0-0} values of J-type P3HT NFs. (A) Several NFs averaged over the entire microscope field-of-view (~15 μm) and (B) a single NF.

Previous theoretical simulations of J-type P3HT aggregates predicted smooth decreases of the PL 0−0/0−1 ratios as temperatures approach 0 K.[12] PL spectra do show nearly monotonic red-shifts and small decreases in the 0−0/0−1 ratios before and after the apparent transition temperature but, the discontinuity observed in both ensemble and single NF spectra is not expected from theory considerations. Significant increases in the overall PL intensity also occur in the characteristic temperature range (see the Supporting Information) which, taken together with changes in line shape parameters, point to a change in P3HT chain packing characteristics.

Unlike their J-aggregate counterparts, H-type NF lineshapes do not exhibit significant temperature dependence and remain mostly H-like over the entire temperature range (see the Supporting Information). Importantly, J-type NFs form over long periods of time, which leads to molecular weight fractionation of P3HT chains and high quality aggregates. However, NFs assembled in anisole form immediately after dissolution of P3HT leading to distinct domains with different chain packing characteristics and greater disorder. These effects are expected to smear out any distinct changes in P3HT packing and order in temperature-dependent PL spectra. Evidence of heterogeneity within these single NFs is also apparent from ensemble spectra of solution anisole NF dispersions (Figure 1A) where PL spectra show weak J-type character and absorption spectra appear distinctly H-like.

The presence of distinct domains within anisole NFs gives rise to interesting PL features in dispersed samples. For example, Figure 4 shows ensemble polarized PL spectra of

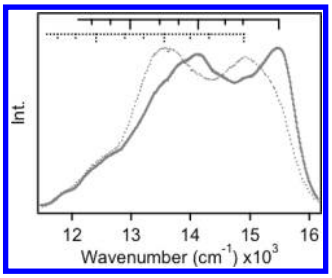

Figure 4. Polarized PL spectra of several anisole assembled P3HT NFs with orthogonal polarizations showing selection of different emitting species.

dilute anisole NFs at 4 K taken over the entire field-of-view that qualitatively demonstrate the presence of multiple aggregate domains with different orientations and transition energies. At least two distinct electronic origin transitions can be discerned with an average separation of ~400−500 cm^{-1}. Similar to J-aggregate emitters, the C=C symmetric stretch (~1450 cm^{-1}) corresponds to the dominant progression forming mode. It is possible that the apparent origin transitions are in fact progressions in lower frequency modes. However, their relative intensities should not have any polarization dependence and we propose that these features are indeed distinct transitions from multiple domains. Unfortunately, the low spectral resolution and overlapping H- and J-type lineshapes make a detailed analysis difficult and ambiguous.

Baghgar et al. recently reported similar behavior where PL spectra of individual NFs displayed multiple apparent origin transitions from both H- and J-type species.[15] Figure 5 shows polarized PL spectra for a single anisole NF at 4 K that may

dx.doi.org/10.1021/jp308586k | J. Phys. Chem. B 2013, 117, 4478−4487

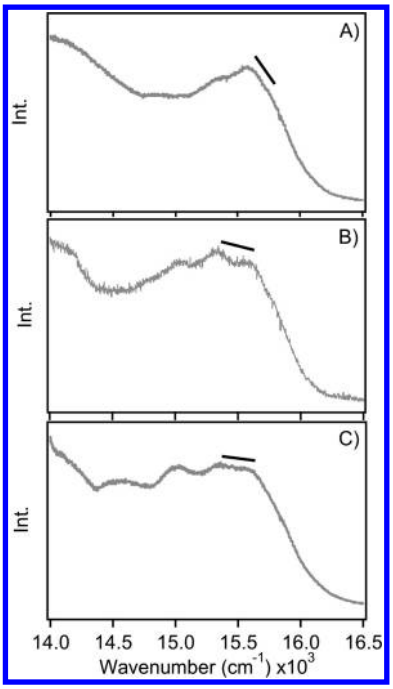

Figure 5. Polarization dependent PL spectra of a single P3HT NF assembled from anisole. (A) 0°, (B) 45°, and (C) 90°. Bars are a guide for the eye to illustrate changes in intensity distributions.

help further unravel the nature of emitting species in these samples. Distinct changes in the apparent electronic origin intensities are observed depending on the angle of the emission polarizer corresponding to photoselection of particular domains. Most spectra show H-aggregate behavior although some J-type emitters were observed (see the Supporting Information) but these had significantly smaller 0−0/0−1 PL intensity ratios than the toluene assembled J-aggregates. Because of the random orientations of the single NFs, the emission polarizer was initially rotated to maximize the intensity of the first resolved peak then subsequently rotated to 45° and 90°. Similar to ensemble PL data, intensity distributions within the vibronic peaks change with the polarization angle. Particle-to-particle heterogeneity was substantial in these spectra again complicating the assignment of the structural origins of each emitter.

It is also possible that the appearance of multiple emitters in anisole NFs correspond to Davydov components originating from nonequivalent sites within the crystalline unit cell. Recent studies have shown that either reformation of NF structures or slow growth from controlled solvent evaporation leads to the coexistence of a new phase (i.e., type I′) from X-ray diffraction patterns and scanning calorimetry studies.[22] This coexistence phenomena could result in distinct lineshapes built on several origins. However, the type I′ phase is of higher crystallinity and the rapid assembly of NFs in anisole solutions implies that coexistence of such a phase is unlikely.

Additional insights into organization of P3HT chains as well as domain orientations can be obtained from excitation polarization modulation experiments that have been used extensively by Barbara and co-workers to study chromophore order within single polymer molecules and aggregates.[23−27] We use excitation polarization-dependent PL imaging to assess the alignment of chromophores within both H- and J-type NF aggregates as well as the existence of aggregate domains with different spatial orientations. In this experiment, the polarization angle of the laser excitation was rotated continuously from 0° to 180° and the change in integrated intensities for single NFs within the field-of-view were recorded. These measurements report the projection of the transition moment x-y components in the laboratory frame and thus the relative orientations of chromophores (chain segments within the aggregate).[26,28] The modulation depth, M, was determined for each particle from the following expression:

$$M = \frac{I_{max} - I_{min}}{I_{max} + I_{min}} \quad (1)$$

and averaged excitation polarization-dependent intensities were fitted to a cosine function, $I \propto 1 + M \cos 2(\theta - \phi)$ where θ and ϕ are the polarization angle and phase, respectively (see the Supporting Information for examples). Figure 6 shows M

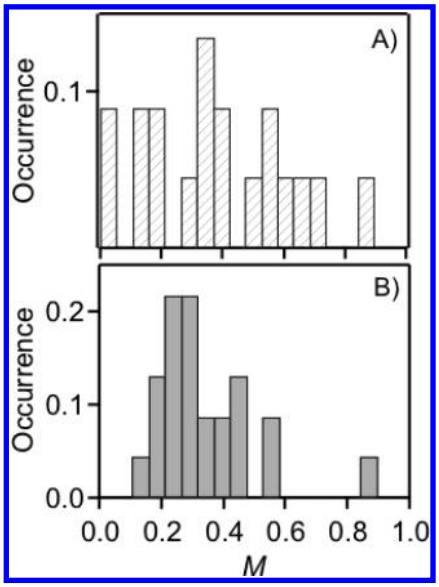

Figure 6. Modulation depth histograms for anisole (A) and toluene (B) NFs.

histograms for anisole (A) and toluene (B) NFs. If chromophores are randomly oriented (isotropic), M values should be small (~0) due to the lack of preferential excitation with varying polarization angle. On the other hand, anisotropic samples have large M values (~1) due to either single dipole type or well-aligned (ordered) chromophores. Interestingly, both NF types have similar average values of ~0.35 although the anisole NFs have a much broader distribution, reflecting the greater disorder within these structures due to variations in size and the presence of multiple domains. The lower M values in J-type NFs were surprising and suggests that chromophores are not well-aligned although intrachain order within these units is high as seen from PL lineshapes. This is likely due to the formation of separate "grains" within the NF structure with different orientations, as was demonstrated recently by single NF electron diffraction data in ref 9. Separate excitation polarization modulation experiments on single J-aggregate NFs obtained in a confocal scanning instrument produced similar average M values and distributions (data not shown) demonstrating that depolarization effects or other instrument contributions have little impact on the observed behavior. Another explanation for smaller than expected M values in J-type NFs is the association (or, agglomeration) of several

dx.doi.org/10.1021/jp308586k | J. Phys. Chem. B 2013, 117, 4478−4487

particles upon dispersion into polystyrene hosts. Although chain packing characteristics within each NF would not likely be significantly affected, the agglomerate would exhibit less polarization selectivity. To test this hypothesis, we compared particle brightness (i.e., PL counts over a specific integration time) and M value for each NF particle. If particles were agglomerating, larger integrated intensities would correspond to smaller M values. However, no discernible dependence between particle size (brightness) and M value was observed (see the Supporting Information). While unlikely, NFs may form hierarchical structures,[29] such as branches or bundles, leading to smaller dichroic effects but particle size estimates from imaging studies (Figure 1) suggest otherwise. NFs could potentially orient perpendicular to the substrate (as was observed previously in single polymer molecules deposited on bare glass) although dispersion in host matrices should lead to random orientations. We conclude that the lower than expected M values for J-type NFs probably originate from grain boundaries within the single NF structures.[9] In the case of the anisole assembled NFs, grains are expected to be larger, possess different chain packing characteristics and greater orientational inhomogeneity.

We have so far demonstrated that temperature-dependent PL spectra of H- and J-type NFs reveal useful insights into the role of chain packing on optical properties. The temperature-dependent J-aggregate PL spectra illustrate that subtle changes in chain packing characteristics due to a small contraction of NF volume can result in significant changes in PL spectra and, hence, intrachain order and exciton coupling. To better understand the susceptibility of P3HT chain packing characteristics to minor perturbations on the NF structure, we perform complementary pressure-dependent PL spectra and lifetimes on both H- and J-type NFs.

Pressure-Induced Increases of Exciton Bandwidths. Time-resolved PL spectroscopy of P3HT thin film aggregates contain contributions from interchain torsional relaxation[17] and self-ionization processes[19] giving rise to nonexponential decay profiles. We previously measured PL lifetimes of P3HT NF J-aggregates along with thin films of both regioregular and regiorandom P3HT that reveal correlations between the amount and type of aggregation on exciton decay signatures.[12] Namely, each sample showed multiexponential lifetime decay profiles with contributions primarily from a fast, instrument-limited component (~50 ps) and a slower decay corresponding to the exciton recombination (~700 ps to 1 ns). Although the time scales of each component did not vary significantly with sample form and type, the amounts of each were correlated to the intrachain order within each sample.

The fast component of P3HT aggregate PL decay has been attributed to interchain torsional relaxation processes within the aggregate and is expected to increase when monomers of neighboring chains in the π-stack have larger torsional disorder that subsequently relax to a planar geometry in the excited state.[17] For example, thin film H-aggregates showed much larger contributions from this fast component (>70%) compared to NF J-aggregates (~40%) suggesting greater torsional rigidity of the P3HT chains in the latter.[12]

We measure combined pressure-dependent PL spectra and lifetimes on both H- and J-type NF's up to ~40 kbar to determine how fast and slow PL decay components change with minor chain packing perturbations. The previously proposed high sensitivity of chain packing and intrachain order in J-aggregate NFs should result in significant changes in pressure-dependent PL lifetimes. Namely, an increase of the fast component contribution owing to greater torsional disorder is expected at higher pressures corresponding to increased H-aggregate character. Figure 7 shows pressure-dependent lifetimes of J-aggregate NFs and decays are fitted using a double exponential model described previously.[12] As pressure increases the contribution of the fast component increases by ~50% at the highest recorded pressure (~25 kbar) presumably due to increased disorder between monomers (i.e., lower intrachain order). PL lineshapes also become more H-like over the pressure range shown in Figure 7 indicating increased interchain exciton bandwidths typical of H-aggregates. Red-shifts and lower yields of the pressure-dependent PL spectra are apparent and consistent with larger exciton bandwidths allowing these species to delocalize over neighboring chains thus increasing the probability that they will find a lower energy emitting site within their lifetime.

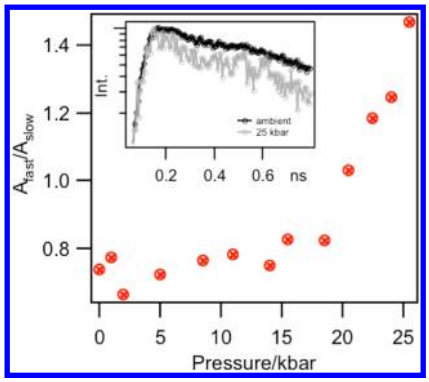

Figure 7. Ratio of amplitudes from the "fast" and "slow" fit components to experimental pressure-dependent PL lifetimes of J-aggregate P3HT NFs. Inset: representative decay traces of NF's at ambient pressure (~1 bar) and ca. 25 kbar.

The data in Figure 7 supports our previous hypothesis that pressure disrupts intrachain order by acting on dangling chains outside the core of the NF aggregate in addition to affecting packing and ordering of P3HT alkyl side groups. The pressure range studied here is also still well below the range in which bond lengths and angles are usually affected and only changes in chain packing characteristics are expected.[30]

Temperature- and Pressure-Induced Repacking of P3HT Alkyl Side Groups. Using a model P3HT aggregate consisting of three chains with 20 monomers each, Niles et al. predicted a continuous transition from J- to H-type behavior at lower temperatures when a nonzero interchain coupling is present.[12] In this framework, interchain coupling effects should become apparent at low temperatures due to a "freezing out" of thermal fluctuations in low frequency intermolecular modes. This situation results in lower dynamic disorder although monomer rings may still possess static disorder, monomer rings may still possess static disorder (i.e., low intrachain order) as is the case for H-type aggregates. As stated above, J-type P3HT NFs are not ideal J-aggregates, and it was determined that a residual interchain coupling exists of ~50—100 cm^{-1}.[12] The aggregate model does not explicitly treat the packing arrangement of alkyl side groups of P3HT that, while being electronically inert, do have a large influence on directing the π-stacking characteristics of the backbones and, consequently, exciton coupling.[31]

dx.doi.org/10.1021/jp308586k | J. Phys. Chem. B 2013, 117, 4478−4487

Variable temperature and pressure induce a small perturbation on the NF structure (i.e., decrease in volume) that alters chain packing characteristics and intrachain order. Specifically, the alkyl side group packing arrangements should be most susceptible to temperature- and pressure-induced changes in side group packing owing to their flexible (compressible) nature. Even small changes in side group packing could cause sufficient reductions in intrachain order and J-aggregate character owing to the established sensitivity between intrachain order and exciton coupling.[2,6,13] It was previously suggested that either a phase transition from a type I (end-on) to a type II (interdigitated) alkyl side group packing or, smaller interchain spacings were responsible for the apparent increase in exciton bandwidths with variable temperature and pressure.[12] Based on earlier pressure-dependent spectroscopy of P3HT films of lower regioregularity and higher polydispersity, pressure planarizes the polymer backbone thus allowing chains to pack more efficiently in the smaller sample volume.[32] Since P3HT chains in the J-aggregate structure should already exist in highly planar conformations, it is doubtful that temperature and pressure result in increased planarity. Instead, we propose that variable temperature and pressure induce a phase transition involving the repacking of P3HT alkyl side groups that decreases intrachain order causing a loss of J-aggregate character. Pressure increases inhomogeneity making abrupt changes in the E_{0-0} and 0−0/0−1 line shape parameters as well as lifetimes for pressure-dependent PL spectra of J-type NFs less apparent.

In order to better understand the sensitivity of J-type NFs to small packing perturbations, it is first necessary to consider the manner of the self-assembly process for both NF types studied. P3HT NFs fabricated in toluene solutions assemble over long time scales (>24 h) and the alkyl side groups of these J-type structures should adopt the lower energy end-on (type I) packing arrangement. In contrast, P3HT NFs assembled in anisole form instantly implying that chains do not have sufficient time to adopt the most energetically favorable side group packing arrangement and probably exist in both end-on and interdigitated configurations.[22,33] This situation is akin to previous rapid quenching studies from polymer melts[34] and, based on single NF PL spectra (Figure 5), arises from the fact that anisole is a poor solvent for P3HT and therefore rapidly forms aggregates to minimize solvent interactions. TEM imaging studies of both types of NF structures show much larger (∼2×) widths for the toluene assembled J-type samples as well as a looser packing arrangements which also supports a type I alkyl side group packing in these NFs.[35] Additionally, powder X-ray studies showed larger interlamellar (100) *d*-spacings of 17.1 Å vs 16.8 Å between J- and H-type NFs, respectively.[9,36] As temperature (pressure) decreases (increases), the NF aggregate structure contracts causing a repacking of the side chains where the alkyl chains switch to an interdigitated mode of packing. In this type II configuration, more torsional disorder (i.e., lower intrachain order) is expected due to steric interactions of the closer-packed side groups likely causing the thiophene units to buckle slightly out-of-plane. As temperature (pressure) is increased (decreased), the structure reverts back to a type I configuration and spectra return to J-like behavior (see the Supporting Information). It is also important to stress that only native J-type NFs possess this ability to switch between dominant intra- and interchain exciton couplings by temperature or pressure-induced alterations in alkyl side group packings.

Short chain alkanes also melt in the same temperature range as the observed transition temperature range in Figure 3A, further supporting a structural phase transition of the P3HT side groups as the origin for temperature-dependent loss of J-aggregate character.[37] Another intriguing explanation is that J-type NFs adopt the type I′ side group packing arrangement mentioned earlier. Recent studies have shown that slow crystallization of P3HT aggregates in chloroform leads to the type I′ structure and heating above ∼54 °C returns the packing to the more common type I arrangement.[38] Because the type I′ structure is considered more ordered, we do not anticipate that J-type NFs could adopt the type I′ configuration at lower temperature and higher pressure.

Interestingly, related temperature-dependent order−disorder transitions have been reported recently in other prototype polymer systems involving a significant change in exciton coupling behavior. For example, Köhler et al. performed temperature-dependent PL and absorption measurements on MEH-PPV chains dispersed in a glassy matrix which showed a transition from predominantly disordered (blue) conformations to ordered (red) ones at ∼200 K.[39] They suggest that, although the red species PL line shape resembles an intrachain J-aggregate exciton (i.e., 0−0/0−1 > 1), formation of this species requires several chains to minimize interactions with the surroundings (solvent).[39] J-type species are also apparent in PL spectra of single MEH-PPV molecules where, instead of multiple chains interacting, the polymer organizes into an aggregate-like structure by folding back onto itself leading to ordered segments capable of supporting an intrachain, J-type exciton.[40−42] Unlike P3HT aggregates, interchain coupling in MEH-PPV is much weaker due to the more sterically hindered and disordered alkoxy side groups that effectively inhibit this interaction. However, thermal annealing treatments promote increased interchain communication in MEH-PPV leading to a loss of J-aggregate character in optical lineshapes,[43,44] similar to the low temperature and high pressure effects on P3HT J-type NFs reported here. As demonstrated in J-aggregates of both MEH-PPV red emitters and P3HT, closely spaced chain segments are required in order to planarize the backbone to accommodate larger intrachain couplings.

Thus far, we have shown that steady-state and time-resolved PL spectroscopy of H- and J-type P3HT NFs are informative for understanding the range of tunability of exciton coupling, they do not reveal faster relaxation processes preceding recombination of thermalized excitons or trapped charges. Similar to PL measurements, these dynamics are expected to have a strong dependence on the chain packing characteristics of the aggregate that affect not only the extent of exciton and polaron delocalization but also their directionality (i.e., intra- or interchain). Moreover, recent ultrafast spectroscopy on P3HT films demonstrated the tendency for autoionization processes to occur at the boundaries of ordered and disordered P3HT regions.[18,19] The confined nature and well-defined boundaries of NF aggregates makes these systems ideal candidates for exploring packing-dependent exciton and polaron dynamics. However, little is presently understood about the roles of domains within these structures on exciton dissociation yields. We now use TAS techniques to study ultrafast excited state relaxation and recombination of both excitonic and polaronic species generated after photoexcitation in H- and J-type P3HT NFs.

Ultrafast Transient Absorption Shows Differences in Intra- and Interchain Exciton Coupling in H- and J-

dx.doi.org/10.1021/jp308586k | J. Phys. Chem. B 2013, 117, 4478−4487

Aggregate NF Suspensions. Transient absorption spectroscopy (TAS) was conducted on solution phase P3HT NF dispersions allowing for the direct study of ultrafast relaxation and recombination dynamics of exciton and polaron species. Both H- and J-type NFs are studied to reveal the influence of NF chain packing characteristics on these dynamics. TAS has several key advantages in the study of polymer aggregates, mainly, these measurements are not affected by self-absorption phenomena as well as residual amorphous P3HT present in the supernatant that often plague steady-state optical measurements. The latter effect is particularly troublesome in the study of J-type NFs and can lead to substantial line shape distortions even at relatively modest concentrations. The TAS data presented herein therefore offer a more reliable determination of the exciton coupling strengths.

Acquired TAS data were analyzed within a sequential global analysis framework[45,46] to yield evolution associated difference spectra (EADS, Figure 8) and kinetic fits (Figure 9). EADS can be interpreted as transient spectra representative of the NF ensemble on a given time scale (see Supporting Information for population trajectories). TAS experiments on solution phase P3HT aggregates generally show two processes: structural relaxation[16,17] and autoionization.[18,19] The crystalline nature of the NF systems limits large scale structural relaxation, so only autoionization and subsequent recombination dynamics significantly contribute to transient absorption (TA) data. Within the visible probed spectral range, three signals are observed (Figure 8): a negative ground state bleach (GSB) at $\lambda < 625$ nm, polaron-pair (PP) at $\lambda = 660$ nm, and delocalized polaron (DP) at $\lambda > 725$ nm.[47] The GSB spectrum effectively mirrors the (inverted) ground state absorption of the excited population. The PP peak corresponds to an intrachain charge transferred species with two loosely correlated, oppositely charged carriers on the same polymer chain (660 nm).[47] The other autoionization product is a DP, which is resolved as the blue side of a broad delocalized polaron absorption feature (Figure 8, $\lambda > 725$ nm).[47] This excited state absorption corresponds to a polaron that has been formed via charge transfer to an adjacent chain thereby yielding interchain $P3HT^{\cdot+}$ and $P3HT^{\cdot-}$.

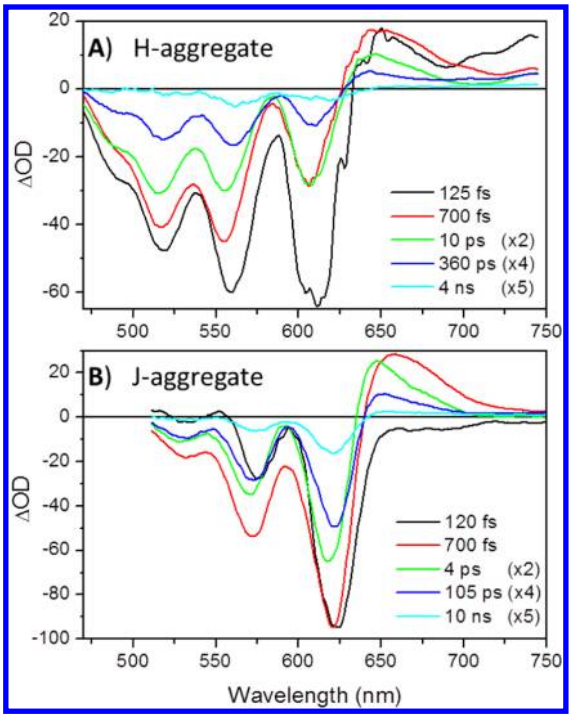

Figure 8. Evolution associated difference spectra (EADS) resultant from global analysis. Each EADS is spectrally representative of the excited state population at a given time (see the Supporting Information for population trajectories). Each population evolves into the next with the listed time constant (legend). EADS are displayed with the same wavelength axis to facilitate comparison.

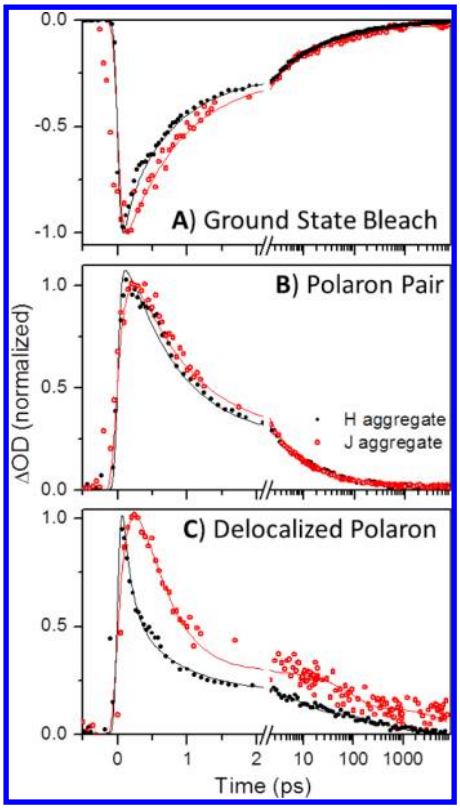

Figure 9. Normalized TA kinetics with global fits for ground state bleach (A, 560 nm (H-type)/650 nm (J-type)), polaron pair (B, 660 nm), and delocalized polaron (C 740 nm) features. Note the linear-logarithm break at 2 ps.

The GSB spectrum effectively isolates the ground state absorption characteristics of the excited NFs by selectively exciting subpopulations in the sample, rather than the ground state absorption (Figure 1), which probes the entire solution ensemble. Most notably, the 0−0/0−1 peak ratios vary greatly for the postvibrational relaxation ($\tau > 125$ fs) GSB (Figure 8, red curves) in H-type (~0.5) and J-type (~2). This can be regarded as the "true" ground state absorption of the NFs in solutions without spectral contamination from possible amorphous P3HT also present in small amounts. The lack of significant amorphous GSB contribution to the signals (roughly a Gaussian peak centered at 450 nm)[16] also confirms that the pump pulse selectively excited only P3HT NF aggregates and all observed dynamics originate from NF excitation. The GSB decay is slightly faster in H-type than J-type NFs for $\tau < 2$ ps (Figure 9A). The global analysis fitting reveals that this apparent difference is due to an increased yield of faster-decaying DP in the H-type aggregate, rather than an actual increase in recombination rates. This is coupled to the PP and DP yield and decay that are discussed below.

dx.doi.org/10.1021/jp308586k | J. Phys. Chem. B 2013, 117, 4478−4487

Due to the intrachain nature of the PP state, it is not expected to display any dependence associated with interchain coupling. It is, however, observed to be extremely sensitive to intrachain order,[15] which is primarily observed in inter- versus intrachain coupling yields. Normalized PP formation and recombination kinetics are nearly identical in H- and J-type NFs (Figure 9B) implying that the intrachain coupling determines PP formation yield, but has little effect on formation and recombination kinetics beyond the first 100 fs.

DP formation via interchain charge transfer is primarily dependent on interchain coupling, which should be similar in both NF types (i.e., similar interchain spacings). However, the formation of DP is in competition with PP species. Assuming that the extinction coefficients for PP and DP bands are comparable in H- and J-type aggregates, the relative peak height of PP versus DP serves as a good indicator of the interplay between inter- and intrachain coupling. The initial PP:DP peak height ratios are 1.5:1 and 10:1, for H-type and J-type, respectively. This effectively shows that the initial formation of intra- versus interchain species is modulated by approximately an order of magnitude by the subtle structural deviation induced by J-type aggregation. Previous ultrafast spectroscopy studies on P3HT films determined that polaron generation processes chiefly occurs at the interface between ordered and disordered P3HT domains.[19] The fact that J-type NFs are almost completely crystalline (aggregated) implies little interface area and therefore consistent with the substantially lower charge transfer yields observed in our data. The normalized DP kinetics (Figure 9C) also shows that the recombination out of the DP state is significantly slower in J-type NFs. This is attributed to improved intrachain coupling allowing the interchain polarons to migrate along their respective chains more efficiently, thereby delaying recombination.

In summary, TA data resolves that the structural differences in H- and J-type P3HT NFs result primarily in modulation of intrachain coupling. This modulation causes an order of magnitude reduction in the relative interchain charge transfer yield in J-type NFs. PP recombination and bleach recovery also show minor kinetic differences due to NF type, while DP recombination is significantly slower in J-type NFs. This is due to improved intrachain coupling for polarons as well as excitons in J-type NFs, which effectively delays polaron (DP) recombination.

CONCLUSIONS

Photophysics of crystalline P3HT NF samples display a remarkable dependence on the specific packing arrangement and intrachain order of polymer chains within the aggregate structure. By studying single NF structures using variable temperature PL spectroscopy, new insights into structural changes causing changes in exciton coupling behavior begin to emerge. J-aggregate NFs transition to H-type behavior at ∼110—130 K due to a reversible repacking of alkyl side groups from type I to type II configurations. Pressure-dependent PL decay profiles support this assignment where increase in the fast decay component demonstrates greater interchain torsional displacements expected for lower intrachain order. TAS measurements of H- and J-type NFs demonstrated distinctly different ultrafast polaron (DP) relaxation and recombination dynamics where J-type NFs showed substantially slower recombination dynamics.

Overall, the physical picture obtained from both steady-state and time-resolved spectra of J-type P3HT NFs indicates that individual chains comprising these structures are electronically isolated and effectively behave as a collective of single molecules. However, the small residual interchain coupling term and close spacing of adjacent chains permits reversible and selective tuning of intrachain order and exciton coupling through small changes in chain packing within the aggregate. This particular feature could potentially be exploited as an optical or electronic switch to control exciton and polaron delocalization in these nanoscale functional forms.

ASSOCIATED CONTENT

Supporting Information

Temperature-dependent PL line shape parameters of single and ensemble P3HT NFs, size-dependent polarization modulation depths, low temperature PL spectra of single anisole NFs, and population trajectories from TAS EADS data. This material is available free of charge via the Internet at http://pubs.acs.org.

AUTHOR INFORMATION

Corresponding Author

*E-mail: jkgrey@unm.edu.

Author Contributions

#These authors contributed equally.

Notes

The authors declare no competing financial interest.

ACKNOWLEDGMENTS

Financial support from the National Science Foundation (CHE-0955242, J.K.G.; CBET-0933435, A.J.M.) and the University of California Energy Institute (UCEI) to D.S.L. is gratefully acknowledged. Edwards Niles is acknowledged for assistance with temperature-dependent PL measurements.

REFERENCES

(1) Spano, F. C. *J. Chem. Phys.* **2005**, *122*, 234701/1−234701/15.
(2) Clark, J.; Silva, C.; Friend, R. H.; Spano, F. C. *Phys. Rev. Lett.* **2007**, *98*, 206406/1−206406/4.
(3) Clark, J.; Chang, J.-F.; Spano, F. C.; Friend, R. H.; Silva, C. *Appl. Phys. Lett.* **2009**, *94*, 163306/1−163306/3.
(4) Spano, F. C.; Clark, J.; Silva, C.; Friend, R. H. *J. Chem. Phys.* **2009**, *130*, 074904/1−074904/16.
(5) Spano, F. C. *Chem. Phys.* **2006**, *325*, 22−35.
(6) Spano, F. C. *Acc. Chem. Res.* **2010**, *43*, 429−439.
(7) Brinkmann, M. *J. Polym. Sci., Part B* **2011**, *49*, 1218−1233.
(8) Samitsu, S.; Shimomura, T.; Heike, S.; Hashizume, T.; Ito, K. *Macromolecules* **2008**, *41*, 8000−8010.
(9) Roehling, J. D.; Arslan, I.; Moulé, A. J. *J. Mater. Chem.* **2012**, *22*, 2498−2506.
(10) Kim, B.-G.; Kim, M.-S.; Kim, J. *ACS Nano* **2012**, *4*, 2160−2166.
(11) Zhao, K.; Xue, L.; Liu, J.; Gao, X.; Wu, S.; Han, Y.; Geng, Y. *Langmuir* **2010**, *26*, 471−477.
(12) Niles, E. T.; Roehling, J. D.; Yamagata, H.; Wise, A. J.; Spano, F. C.; Moulé, A. J.; Grey, J. K. *J. Phys. Chem. Lett.* **2012**, *3*, 259−263.
(13) Yamagata, H.; Spano, F. C. *J. Chem. Phys.* **2012**, *135*, 054906/1−054906/12.
(14) Yamagata, H.; Norton, J.; Hontz, E.; Olivier, Y.; Beljonne, D.; Bredas, J. L.; Silbey, R. J.; Spano, F. C. *J. Chem. Phys.* **2011**, *134*, 204703/1−204703/11.
(15) Baghgar, M.; Labastide, J.; Bokel, F.; Dujovne, I.; McKenna, A.; Barnes, A. M.; Pentzer, E.; Emrick, T.; Hayward, R.; Barnes, M. D. *J. Phys. Chem. Lett.* **2012**, *3*, 1674−1679.
(16) Busby, E.; Carroll, E. C.; Chinn, E. M.; Chang, L.; Moulé, A. J.; Larsen, D. S. *The J. Phys. Chem. Lett.* **2011**, *2*, 2764−2769.
(17) Parkinson, P.; Muller, C.; Stingelin, N.; Johnston, M. B.; Herz, L. M. *J. Phys. Chem. Lett.* **2010**, *1*, 2788−2792.

(18) Zhang, W.; Hu, R.; Li, D.; Huo, M.-M.; Ai, X.-C.; Zhang, J.-P. *J. Phys. Chem. C* **2012**, *116*, 4298−4310.
(19) Paquin, F.; Latini, G.; Sakowicz, M.; Karsenti, P.-L.; Wang, L.; Beljonne, D.; Stingelin, N.; Silva, C. *Phys. Rev. Lett.* **2011**, *106*, 197401/1−197401/4.
(20) Piermarini, G. J.; Block, S.; Barnett, J. D.; Forman, R. A. *J. Appl. Phys.* **1975**, *46*, 2774.
(21) Carroll, E. C.; Compton, O. C.; Madsen, D.; Osterloh, F. E.; Larsen, D. S. *J. Phys. Chem. C* **2008**, *112*, 2394−2403.
(22) Pal, S.; Nandi, A. K. *Macromolecules* **2003**, *36*, 8426−8432.
(23) Hu, D. H.; Yu, J.; Wong, K.; Bagchi, B.; Rossky, P. J.; Barbara, P. F. *Nature* **2000**, *405*, 1030−1033.
(24) Adachi, T.; Brazard, J.; Ono, R. J.; Hanson, B.; Traub, M. C.; Wu, Z.-Q.; Li, Z.; Bolinger, J. C.; Ganesan, V.; Bielawski, C. W.; Vanden Bout, D. A.; Barbara, P. F. *J. Phys. Chem. Lett.* **2011**, *2*, 1400−1404.
(25) Traub, M. C.; Lakhwani, G.; Bolinger, J. C.; Vanden Bout, D.; Barbara, P. F. *J. Phys. Chem. B* **2011**, *115*, 9941−9947.
(26) Vogelsang, J.; Brazard, J.; Adachi, T.; Bolinger, J. C.; Barbara, P. F. *Angew. Chem., Int. Ed.* **2010**, *50* (2257−2261), S2257/1−S2257/7.
(27) Grey, J. K.; Kim, D. Y.; Norris, B. C.; Miller, W. L.; Barbara, P. F. *J. Phys. Chem. B* **2006**, *110*, 25568−25572.
(28) Traub, M. C.; Vogelsang, J.; Plunkett, K. N.; Nuckolls, C.; Barbara, P. F.; Vanden Bout, D. A. *ACS Nano* **2012**, *6*, 523−529.
(29) Kamps, A. C.; Fryd, M.; Park, S.-J. *ACS Nano* **2012**, *6*, 2844−2852.
(30) Dreger, Z. A.; Yang, G.; White, J. O.; Drickamer, H. G. *J. Phys. Chem. B* **1997**, *101*, 9511.
(31) Darling, S. B.; Sternberg, M. *J. Phys. Chem. B* **2009**, *113*, 6215−6218.
(32) Hess, B. C.; Kanner, G. S.; Vardeny, Z. *Phys. Rev. B* **1993**, *47*, 1407−11.
(33) Malik, S.; Nandi, A. K. J. *Polym. Sci. B* **2002**, *40*, 2073−2085.
(34) Wang, Y.; Archambault, N.; Belcher, A. M.; Busse, D.; Damon, D. B.; Mills, A.; Riddle, A. E.; Samardjiev, I. J.; Lucht, B. L.; Euler, W. B. *Macromolecules* **2008**, *41*, 7115−7121.
(35) Gao, J.; Kamps, A.; Park, S.-J.; Grey, J. K. *Langmuir* **2012**, *28*, 16401−16407.
(36) Roehling, J. D.; Moulé, A. J.; Arslan, I. *Microsc. Microanal.* **2011**, *16*, 1362−1363.
(37) Garreau, S.; Leclerc, M.; Errien, N.; Louarn, G. *Macromolecules* **2003**, *36*, 692−697.
(38) Yuan, Y.; Zhang, J.; Sun, J.; Hu, J.; Zhang, T.; Duan, Y. *Macromolecules* **2012**, *44*, 9341−9350.
(39) Koehler, A.; Hoffmann, S. T.; Baessler, H. *J. Am. Chem. Soc.* **2012**.
(40) Kim, D. Y.; Grey, J. K.; Barbara, P. F. *Synth. Met.* **2006**, *156*, 336−345.
(41) Yu, J.; Hu, D.; Barbara, P. F. *Science* **2000**, *289*, 1327−1330.
(42) Schindler, F.; Lupton, J. M. *ChemPhysChem* **2005**, *6*, 926−934.
(43) Nguyen, T.-Q.; Doan, V.; Schwartz, B. J. *J. Chem. Phys.* **1999**, *110*, 4068−4078.
(44) Nguyen, T.-Q.; Martini, I. B.; Liu, J.; Schwartz, B. J. *J. Phys. Chem. B* **2000**, *104*, 237−255.
(45) Thibert, A.; Frame, F. A.; Busby, E.; Holmes, M. A.; Osterloh, F. E.; Larsen, D. S. *J. Phys. Chem. Lett.* **2011**, *2*, 2688−2694.
(46) van Stokkum, I. H. M.; Larsen, D. S.; van Grondelle, R. *Biochim. Biophys. Acta* **2004**, *1657*, 82−104.
(47) Guo, J.; Ohkita, H.; Benten, H.; Ito, S. *J. Am. Chem. Soc.* **2009**, *131*, 16869−16880.